



The response of terrestrial ecosystem carbon cycling under different aerosol-based radiation management geoengineering

Hanna Lee¹, Helene Muri², Altug Ekici^{1,3,4}, Jerry Tjiputra¹, and Jörg Schwinger¹

¹NORCE Norwegian Research Institute, Bjerknes Centre for Climate Research, Bergen, Norway

²Industrial Ecology Programme, Department of Energy and Process Engineering, Norwegian University of Science and Technology, Trondheim, Norway

³Current address: Climate and Environmental Physics, Physics Institute, University of Bern, Bern, Switzerland

⁴Current address: Oeschger Centre for Climate Change Research, University of Bern, Bern, Switzerland

Correspondence: Hanna Lee (hanna.lee@norceresearch.no)

Abstract. Geoengineering has been discussed as a potential option to offset the global impacts of anthropogenic climate change, and at the same time help reach global temperature targets of the Paris Agreement. Before any implementation of geoengineering, however, the complex natural responses and consequences of such methods should be fully understood to avoid any unexpected and potentially degrading impacts. Here we assess the response of different terrestrial biomes in their ecosystem carbon exchange and storage under three different aerosol-based radiation management (RM) methods applied on top of the baseline RCP8.5 scenario using an Earth System Model (NorESM1-ME). All three methods used in this study (stratospheric aerosol injection, marine sky brightening, cirrus cloud thinning) target the global mean radiation balance at the top of the atmosphere to that of the RCP4.5 scenario. The three different RM methods investigated in this study exhibit vastly different precipitation patterns especially in the tropical forest biome due to the methodological differences in how the aerosols are applied. This resulted in large variability in global vegetation carbon uptake and storage across the three methods as tropical forest biome contribute the largest to global vegetation carbon uptake and storage. Our findings show that there are unforeseen regional consequences in the biogeochemical cycles under geoengineering and these consequences should be taken into account in future climate policies. Although, changes in temperature and precipitation play a large role in vegetation carbon uptake and storage, our results show that CO₂ fertilization also plays a considerable role. We find that changes in vegetation carbon storage under geoengineering application was much smaller than what is exhibited under RCP4.5 scenario that uses climate mitigation efforts by afforestation in the tropics. Hence, it would be important to consider the multiple combined effects and responses of land biomes when applying different strategies to reach the global temperature targets of the Paris Agreement.

1 Introduction

The Paris Agreement, adopted under the Convention of the Parties of United Nations Framework Convention on Climate Change (UNFCCC) in 2015, aims to limit the temperature increase to 2°C, and strive for 1.5°C above pre-industrial levels (UNFCCC, 2015). Reaching global climate targets of 1.5-2°C is very ambitious considering the rate of current warming as such goals require not only strong mitigation efforts (e.g., Rogelj et al., 2016, 2018; van Vuuren et al., 2018), but also negative



emission technologies or carbon dioxide removal (CDR) are likely needed (IPCC, 2018). Geoengineering has been discussed as a potential option to offset the global impacts of anthropogenic climate change, and at the same time help reach those global temperature targets. The complex natural responses and consequences of such methods, however, should be fully understood before implementation of geoengineering to avoid any unexpected and potentially degrading impacts.

By definition, geoengineering is a deliberate attempt to modify the climate system on a sufficiently large scale to alleviate the impacts of climate change (Crutzen, 2006). Two broad categories of geoengineering, which have been discussed persistently in the fifth assessment report of the Intergovernmental Panel on Climate Change (IPCC, 2013), are Carbon Dioxide Removal and Solar Radiation Management (SRM). CDR methods aim at capturing CO₂ from the atmosphere and storing it in reservoirs, where it stays isolated from the atmosphere for a significant period of time. This could be done in a number of different ways, from afforestation to direct air capture of CO₂ with long-term geological storage (Lawrence et al., 2018). SRM methods, on the other hand, aim at modifying the atmospheric radiative budgets by reducing the amount of solar radiation reaching the Earth's surface to alleviate anthropogenic global warming. We hence refer to these methods as radiation management (RM) in this study, as in Schäfer et al. (2015).

Due to the long thermal inertia in the climate system and limitations in maximum removal rate of CO₂, CDR would likely require longer time to lower global temperatures (Zickfeld et al., 2017). On the other hand, several proposed RM methods could stabilize or even reduce global temperature within a few years (Lawrence et al., 2018). The benefits of RM methods may not only be in reducing the current rate of increase in atmospheric temperatures, but also in mitigating climate extremes likely caused by warming (Irvine et al., 2019). Despite this encouraging potential, studies have shown numerous undesirable climatic and biophysical side effects of RM particularly related to sudden termination of RM (e.g., Keller et al., 2014; Lauvset et al., 2017; Lee et al., 2019; Robock et al., 2009; Tjiputra et al., 2016). These studies point out that upon sudden termination of RM, the climate system will return to its "unmitigated" state within a few decades. This may lead to very large rates of change in the climatic state, unless atmospheric CO₂ concentrations are not dealt with during such a RM deployment period. Nevertheless, our understanding on how RM influence vegetation carbon dynamics at regional scales remains limited, with only a few studies published, with focus on single or simplistic RM methods (Dagon and Schrag, 2019; Muri et al., 2014, 2018; Naik et al., 2003; Tjiputra et al., 2016).

In this study, we assess the response of different biomes in their ecosystem carbon exchange and storage under three different RM methods using an Earth System Model. The three RM methods considered in this study are stratospheric aerosol injection (SAI), marine sky brightening (MSB), and cirrus cloud thinning (CCT). These three experiments are described in detail in the Methods section following Muri et al. (2018). In summary, all three are aerosol-based RM methods that have been designed to reduce the level of radiative imbalance at the top of the atmosphere resulting from a high CO₂ emissions scenario (RCP8.5) to those projected for the medium CO₂ emissions scenario, RCP4.5. The mechanism how different methods stabilize the climate are slightly different. The modeling study by Muri et al. (2018) demonstrates that all three of these methods could potentially stabilize atmospheric temperature and reduce net radiative forcing on climate; however, side effects may exist as these methods may alter atmospheric circulation and precipitation patterns. Geoengineering Model Intercomparison Project (GeoMIP, Kravitz et al. (2015)) studies show that there is substantial regional climate variation in response to different methods, scenarios, and



models (e.g., Stjern et al., 2018; Wei et al., 2018; Yu et al., 2015). As a result, different terrestrial ecosystems exhibit varying patterns in vegetation production (NPP). Analyses in vegetation responses show that global mean and high latitude NPP have different patterns (Jones et al., 2013; Lee et al., 2019). This is likely due to different RM methods resulting in different patterns of precipitation in particular. In addition to temperature and precipitation, different biomes are limited by different environmental factors, such as growing season length, dry season length, availability of sunlight for photosynthesis, and soil fertility.

This led us to investigate the following questions: 1) What are the key factors affecting future vegetation under different RM applications? 2) If there are regional differences in the environmental change under RM application, which terrestrial biomes are affected the most in ecosystem carbon uptake and storage? 3) What is the impact of geoengineering termination on terrestrial vegetation and carbon storage? 4) What are the effects of RM applications in global vegetation compared to lower emissions and mitigation scenario (RCP4.5)?

1.1 Model description (NorESM)

We conducted three different aerosol-based geoengineering experiments using the fully coupled NorESM1-ME, where we investigated the impacts of idealized scenarios of aerosol-based geoengineering under a high-CO₂ RCP8.5 and the target temperature scenario RCP4.5 future scenarios. NorESM1-ME is based on the Community Earth System Model (CESM; Gent et al., 2011). Some of the key differences in NorESM1-ME from CESM are: (1) a more sophisticated tropospheric chemistry-aerosol-cloud scheme (Kirkevag et al., 2013), (2) a different ocean circulation model based on the Miami Isopycnic Coordinate Ocean Model (MICOM) with extensive modifications (Bentsen et al., 2013), and (3) the ocean biogeochemical model, which originated from the Hamburg Oceanic Carbon Cycle (HAMOCC) model (Tjiputra et al., 2013). Both the land and atmospheric components have a horizontal resolution of 1.9° latitude × 2.5° longitude, with 26 vertical levels in the atmosphere, whereas the ocean model employs a displaced pole grid with a nominal ~1° resolution with 53 isopycnal layers.

The land component of NorESM1-ME is CLM4 (Lawrence et al., 2011). The land carbon cycle module in CLM4 includes carbon-nitrogen (CN) coupling that is prognostic in CN as well as vegetation phenology; thus, in addition to temperature and precipitation, plant photosynthesis is also limited by the nitrogen (N) availability (Thornton et al., 2009). Sources and sinks of mineral N are implemented in the form of atmospheric deposition, biological N fixation, denitrification, leaching, and losses due to fire events. The plant functional types (PFTs) and land cover change distribution in CLM4 is prescribed and updated annually according to the Coupled Model Intercomparison Project phase 5 (CMIP5) global land use and land cover change data set (Lawrence et al., 2011, 2012). The transient PFT and land cover fields take into account historical and future climate change under RCP8.5 scenario (1850-2100), which were implemented using the harmonized land use change scenarios and Integrated Assessment Model, respectively. Details on PFT, terrestrial carbon and nitrogen cycling, and land cover implementation in the CLM4 model are described in Lawrence et al. (2011). For this study, NorESM is run with fully interactive prognostic carbon cycle (i.e. in emission driven mode).



90 1.2 Aerosol-based geoengineering experiments

Two of the RM methods used in this study aim to reduce the amount of solar radiation reaching the surface to alleviate global warming through spraying of aerosols into the atmosphere, such as stratospheric aerosol injection (SAI) (e.g., Crutzen, 2006; Robock, 2016), and marine sky brightening (MSB) (Ahlm et al., 2017; Latham, 1990). Another technique, called cirrus cloud thinning (CCT) (Storelvmo et al., 2013), aims at increasing the amount of outgoing thermal radiation to space, by reducing the cover of high level ice clouds. Increasing application of RM was used to lower the total radiative forcing in the RCP8.5 baseline simulation down to a temperature level corresponding to RCP4.5, as described in Muri et al. (2018) and similar to the G6sulfur experiment of GeoMIP (Kravitz et al., 2015). The RM is started in year 2020 on the background of the RCP8.5 scenario and continued until the end of the century. The mean of three ensemble members were used for each case. In year 2101 the RM was ended. One ensemble member was extended for another 50 years for each case, such that effects of sudden termination of large-scale RM may be assessed.

The aerosol-based RM experiments were implemented as follows:

1.2.1 Stratospheric aerosol injections (RCP8.5 + SAI)

Since there is no interactive stratospheric aerosol scheme in NorESM1-ME, stratospheric aerosol properties were prescribed based on the approach of Tilmes et al. (2015). In simulations with the ECHAM5 model, sulfur dioxide was released at ~2 km altitude (60 hPa) in a grid box at the equator. The interactive aerosol microphysics module within the general circulation model of ECHAM5 (Niemeier et al., 2011) calculated the resulting distribution of sulfate aerosols in the stratosphere. The aerosol optical depth and distribution represented by the zonal aerosol extinction, single-scattering albedo, and asymmetry factors, were implemented in NorESM1-ME, and are described in more detail in Niemeier and Timmreck (2015). A number of test runs were performed to establish how much aerosols were needed to offset the anthropogenic radiative forcing between RCP8.5 and RCP4.5. The resulting aerosol layer correspond to equivalent emissions of 5 Tg(S) yr⁻¹ in 2050, 10 Tg(S) yr⁻¹ in 2075 and as much as 20 Tg(S) yr⁻¹ in 2100.

1.2.2 Marine sky brightening (RCP8.5 + MSB)

The sea salt emissions parameterisation in NorESM1-ME is coupled to the cloud droplet number concentrations. In this way, the emissions of sea salt may interact with cloud processes, including brightening effects. Emissions of sea salt aerosols were uniformly increased between latitudes of ±45°. This follows the approach of Alterskjær et al. (2013) and the emissions are increased over a wider latitude band to achieve an effective radiative forcing of -4 W m⁻² more readily. The medium sized aerosol bin has been found to be most efficient at brightening clouds in NorESM (Alterskjær and Kristjánsson, 2013). Aerosol emissions were hence increased for the accumulation mode size, with a dry number modal radius of 0.13 μm, geometric standard deviation of 1.59, corresponding to a dry effective radius of 0.22 μm. Sea salt emission increases were of the order of 460 Tg yr⁻¹ at the end of the century.



1.2.3 Cirrus cloud thinning (RCP8.5 + CCT)

With regards to cirrus cloud thinning, the Muri et al. (2014) method was used. The fall speed of all ice crystals at temperatures below -38°C was increased. This is a typical temperature for homogeneous freezing to start occurring. The coverage of ice clouds in the CMIP5 ensemble was assessed by Li et al. (2012), and NorESM was found to perform reasonable compared to satellite observations and indeed one of the better-performing models. The terminal velocity of ice was increased by a factor of 10 by 2100, i.e. within the observational range (Gasparini et al., 2017; Mitchell, 1996).

1.2.4 Analysis of biomes

We follow the definition of different land biomes as in Tjiputra et al. (2016), where plant functional types (PFT) in the CLM4 that represent certain biomes are merged together (e.g. Boreal forest biome includes boreal needleleaf evergreen tree, boreal needleleaf deciduous tree, boreal broadleaf deciduous tree, and boreal broadleaf deciduous shrub PFTs in the CLM4). The biomes are static by taking a 20 year mean (1981-2000) of PFT distribution from the surface dataset. See Supplementary Information 1 for overall distribution of the biomes used in this study. We note that projected land use change characteristics are very different in RCP8.5 and RCP4.5 (Hurt et al., 2011). While there is an increase in cropland and grassland (driven by food demand of an increasing population) at the expense of forested land in RCP8.5, there is an increasing area of forest due to assumed reforestation programs in the mitigation scenario RCP4.5 (van Vuuren et al., 2011).

2 Results and Discussion

2.1 Global scale responses under RM applications

The three RM methods alter the direct visible radiation (DVR) and diffuse visible radiation (FVR) in different directions, with little impact on the level of atmospheric CO_2 concentrations (Figure 1). The differences in direct and diffuse radiation is attributed to how the radiation management methods are implemented, where each differs in affecting longwave and shortwave radiation (Muri et al., 2018). Regardless of the methodological differences, all RM methods are able to reduce the net radiation at the top of the atmosphere and the global mean air temperatures close to the RCP4.5 level as expected. Global land surface air temperature (TSA) increases at a slower rate until the end of the 21st century under all three RM scenarios compared to the baseline RCP8.5 scenario, where there is approximately 2.3°C difference between RM and non-RM world at year 2100. The precipitation patterns altered by RM application, however, are more variable across different RM methods applied. While under CCT application the increase in global precipitation is somewhat higher than RCP8.5 as explained in Muri et al. (2018), SAI shows a reduced rate of increase in global precipitation similar to RCP4.5. Under MSB application, the rate of global precipitation increase falls in between the SAI and CCT. In particular, MSB tends to increase precipitation over extratropical land more than SAI due to the regional application of the forcing (Alterskjær et al., 2012). On the contrary, the CCT keeps the level of precipitation close to RCP8.5 until the year 2100 due to amplified hydrological cycle from increased latent heat flux



(Kristjánsson et al., 2015). The varying precipitation patterns may result in the responses of global scale carbon uptake and release.

There is a large overall increase in global mean NPP until the end of the 21st century in the RCP8.5 scenario and under the three RM scenarios (Figure 1), whereas only a small increase in NPP was simulated under the RCP4.5 scenario. At the same time, there was a large increase in the rate of soil organic matter decomposition (heterotrophic respiration: HR) in the RCP8.5 based experiments. The relatively small NPP difference between RCP8.5 and the RM simulations versus the large differences between those simulations and RCP4.5 illustrates that the CO₂ fertilization effect is much larger in regulating NPP than the effects of temperature and precipitation as the level of temperature and (in the case of SAI and MSB) precipitation are similar between the RCP4.5 scenario and the three RM methods on a global scale. Increase in diffuse radiation and decrease in direct radiation under SAI is expected to increase plant photosynthesis (Mercado et al., 2009), however, these differences across the three different methods do not seem to affect NPP as much as temperature and precipitation at the global level.

2.2 Regional differences in temperature and precipitation

The global spatial patterns of precipitation and NPP towards the end of the century (mean of 2070-2100) show that the differences in precipitation in the three RM methods occur largely in the tropics and extra-tropics (Figure 2). CCT generally increases precipitation in the tropics relative to RCP8.5, whereas SAI decreases precipitation in the same region. Precipitation in MSB mostly increases within the tropical region.

Partitioning of the effects under different RM methods in different land biomes of the world show that there is no noticeable difference in mean annual temperature across the three different RM methods (Figure 3). The cooling imbalance across the three RM forcings exist, where the tropics tend to cool more than high latitudes and is more pronounced in the ocean than on land, with a stronger southern hemispheric cooling for CCT (Muri et al., 2018). We show that precipitation patterns vary across the three methods in different biomes. In all biomes, SAI application results in the largest decrease in precipitation followed by MSB, and CCT relative to RCP8.5 scenario. The precipitation differences across the three methods are large, particularly in the tropics and the mid-latitudes, where CCT application results in higher precipitation rates than the two other methods. The difference in precipitation becomes amplified over time until the end of the 21st century. According to Muri et al. (2018), shortwave radiation based geoengineering methods exhibit strong reductions in global precipitation levels relative to RCP8.5, but also relative to RCP4.5. CCT leads to a slight increase of global precipitation even over RCP8.5 levels; however, land precipitation patterns in different biomes vary. Aggregated over all biomes, precipitation changes are much smaller than over the total (ocean+land) area. Particularly, precipitation is not reduced below RCP4.5 levels for SAI and MSB as in Muri et al. (2018) (compare their Figure 2 with Figure 1 in this study).

2.3 Biome specific carbon uptake and release rate

The NPP in the three methods follow similar spatial patterns as the precipitation and are highly correlated as expected (Supplementary Information 2). Among the three RM simulations, SAI and MSB exhibit negatively deviating global NPP over time from the baseline RCP8.5 scenario until the termination of RM at the end of the 21st century (Figure 1). This pattern



is dominated largely by three biomes: tropical forest, grass-shrubland, and temperate forest (Figure 4). NPP and microbial
185 respiration (HR) in MSB and SAI simulations negatively deviate from the RCP8.5 simulation, whereas in CCT both remain at
a similar level to the RCP8.5 in the tropical forest, grass-shrubland, and temperate forest likely due to increased precipitation
level in these biomes. But since temperature is a stronger regulator of NPP and HR in high latitude biomes, CCT simulations
also exhibit decreased NPP and HR there compared to the RCP8.5 scenario.

Application of RM altered temperature and precipitation patterns globally, there was no change in seasonality between the
190 three RM methods to the baseline RCM8.5 scenarios, where the changes in temperature and precipitation were only in the
magnitude. As a result, we did not observe any noticeable changes in seasonality for NPP and LAI between RM and RCP8.5
scenario (Supplementary Information 3 and 4) as seen in Dagon and Schrag (2019).

2.4 Biome specific carbon storage

Vegetation carbon storage in different biomes illustrate that global vegetation carbon storage changes are dominated by the
195 responses in tropical forest biome (Figure 5). Under the baseline RCP8.5 scenario, global vegetation carbon storage decreases
due to reduced tropical and temperate forest and grass-shrubland area as part of the land use change scenario used in the
RCP8.5 scenario (Riahi et al., 2011). Compared to the baseline RCP8.5 scenario, vegetation carbon in Arctic tundra, boreal
forest, and tropical forest biomes are affected the most under RM application. In Arctic tundra and boreal forest biomes,
all three RM scenarios result in a slightly reduced accumulation in vegetation carbon compared to RCP8.5 scenario likely
200 due to decreased temperature exhibiting the temperature limitation in high latitude biomes. In tropical forest, SAI application
reduces vegetation carbon storage relative to the RCP8.5 scenario, but CCT application slightly increases carbon storage due
to increased precipitation (Figure 2). The magnitude of change in global vegetation carbon at the end of the century due to
application of different RM methods are up to 10 PgC, whereas the magnitude of vegetation carbon reduced in the 80 year
simulation due to the different underlying land use change scenarios in RCP4.5 and RCP8.5 is up to 100 PgC (Figure 5,
205 Supplementary Information 6), due to increased forest and grassland area used as part of the RCP4.5 scenario (Thomson et al.,
2011). This highlights that large scale changes in vegetation carbon storage depends much more on anthropogenic land use
change than on additional perturbations caused by application of RM in our simulations.

In tropical forest, the differences in vegetation carbon storage appeared to be correlated to precipitation patterns, where de-
crease and increase in precipitation in the three different methods regulate vegetation carbon storage. Differences in vegetation
210 and soil carbon storage in temperate zone (temperate forest and grass-shrubland), however, did not always correspond directly
to varying precipitation patterns. For instance, approximately 100-120 mm difference in mean annual precipitation shown in
temperate forest and grass-shrubland biomes between SAI and CCT methods do not portray into differences in vegetation car-
bon storage (Figure 3, Supplementary Information 5). This likely due to increased respiration rate overshadowing the increase
in NPP (Figure 4).



215 2.5 Effects of RM termination

Upon sudden termination of RM application, the level of radiation, temperature, and precipitation quickly converge to the baseline RCP8.5 scenario (Figures 1, 3, 4). Note that the temperature does not increase to exactly the same level as the RCP8.5 scenario, which has been observed in previous studies and is due to the thermal inertia of ocean heat uptake (Tjiputra et al., 2016). As the temperature and precipitation patterns converge towards the RCP8.5 scenario, NPP also becomes similar to the RCP8.5 scenario (Figure 1). The soil carbon storage decreases as RM is terminated and towards the end of the simulation in year 2150, soil carbon storage in all three RM methods are at a similar level (Supplementary Information 5), but the magnitude is still higher than under the RCP8.5 scenario by 10 PgC globally. The likely accumulation of soil carbon under RM application may be viewed as one of the positive effects of geoengineering, however, the magnitude of the offset between carbon loss in vegetation carbon storage and accumulation of soil carbon storage should be investigated with an updated and more comprehensive version of the model. Globally, land carbon accumulation associated with RM would remain on land for at least 50 years following termination (Muri et al., 2018). Although the termination effects seem catastrophic due to its rapidity in particular, some studies suggest that realistically the most extreme cases would be unlikely as termination could be avoided by geopolitical agreement once deployed (Parker and Irvine, 2018).

2.6 Implications and limitations

Reduced atmospheric temperature and precipitation under RM have large effects on vegetation carbon storage compared to the baseline scenario, RCP8.5. Under the RCP4.5 scenario, the rate of carbon uptake is slower due to reduced temperature, precipitation, and atmospheric CO₂ levels (Figure 1). However, global vegetation carbon storage is far greater than the RCP8.5 and the three RM simulations, which are based on underlying RCP8.5 scenario assumptions (Figure 5), due to the larger forest and grassland areas in the RCP4.5 scenario (Thomson et al., 2011). As a result, the difference in global vegetation carbon between the RCP4.5 scenario and the rest of the RCP8.5 based scenarios is nearly 170 PgC. This strongly suggests that on a global scale, the areal change of vegetation and land surface management play very important roles when accounting for the global scale vegetation carbon storage. We suggest taking this point into account when comparing the different pros and cons of technological applications such as geoengineering and mitigation options such as afforestation.

Our results suggest that even with reduced temperature stress created by RM application, productivity of vegetation in the three most productive biomes on Earth may be reduced due to changing precipitation patterns (particularly SAI). This implies that RM may have negative effects on food production globally as tropics and temperate climate zone combined are the largest food producing areas on the globe (Ramankutty and Foley, 1999). Although not directly investigated in this study, different RM methods have shown various climate extremes as well as mitigating them, which will have profound effects on the physiology of vegetation (Aswathy et al., 2015). Indeed, some studies show seasonal variation in temperature under geoengineering (Dagon and Schrag, 2019), although we did not observe this in our study. This is not within the scope of our study, but could be an interesting point to consider in future studies.



We acknowledge that CLM4 has numerous limitations that prevents it from accurately estimating global scale soil carbon storage, and therefore, we do not make an estimation of global soil carbon storage. But here, we compare soil carbon storage under different methods to understand the factors controlling the difference across the three RM methods. Soil carbon storage increases under RM application compared to the baseline RCP8.5 scenario (Supplementary Information 5 and 6), because the decrease in temperature slows the rate of soil organic matter decomposition by microorganisms. An increase in total soil carbon is also simulated under the RCP4.5 scenario. In different biomes, temperate forest exhibits the largest difference across the three RM methods, where soil carbon storage under SAI method is nearly 1.0 Pg carbon higher than CCT at the end of the 21st century. This is likely due to lower precipitation in SAI, which reduced the rate of decomposition.

255 3 Conclusions

We show that the three different RM application mainly differ in the precipitation patterns, which in turn affect differences in global scale NPP. The precipitation differences across the three RM application are the most pronounced in the tropics and mid-latitudes, where SAI application results in the largest decrease in precipitation followed by MSB, and CCT relative to RCP8.5 scenario. Tropical forest shows largest variability in NPP and vegetation carbon storage as the precipitation patterns vary the most across the three methods in the tropics compared to other biomes. Ultimately, all three RM applications investigated in this study reduced the surface temperature to the level of RCP4.5 scenario with vegetation carbon uptake and storage being affected due to different temperature and precipitation patterns created by the different RM methods. Our results illustrate that there are regional differences in the biogeochemical cycles under application of large scale RM and suggest that such effects should be taken into consideration in future shaping of climate policies. Although changes in temperature and precipitation plays a large role in vegetation carbon storage capacity, CO₂ fertilization plays a considerable role in terrestrial carbon dynamics that can overshadow the effects of temperature and precipitation. Furthermore, changes in vegetation carbon storage under large-scale RM application was much smaller than that exhibited under RCP4.5 scenario, which uses climate mitigation efforts by afforestation in the tropics. Hence, it would be important to consider the multiple combined effects and responses of land biomes when applying different strategies to reach the global temperature targets of the Paris Agreement.

270 *Data availability.* The model simulations used in this study are archived and available at the Norwegian Research Data Archive server (<https://doi.org/10.11582/2019.00007>).

Author contributions. HM and JT received funding; HM and JT designed and conducted simulations; HL and AE analyzed the data; HL, HM, and JS wrote the manuscript; all authors contributed to editing of the manuscript

Competing interests. There are no competing interests present.



Acknowledgements. This research was supported by the Research Council of Norway projects EXPECT (229760/E10), EVA (229771), and HiddenCosts (268243); Bjerknes Centre for Climate Research strategic project SKD-LOES. The simulations were performed on resources provided by UNINETT Sigma2 - the National Infrastructure for High Performance Computing and Data Storage in Norway, accounts nn9182k, nn9448k, NS2345K, and NS9033K.



280 References

- Ahlm, L., Jones, A., Stjern, C. W., Muri, H., Kravitz, B., and Kristjánsson, J. E.: Marine cloud brightening - as effective without clouds, *Atmospheric Chemistry and Physics*, 17, 13 071–13 087, <https://doi.org/10.5194/acp-17-13071-2017>, 2017.
- Alterskjær, K. and Kristjánsson, J. E.: The sign of the radiative forcing from marine cloud brightening depends on both particle size and injection amount, *Geophysical Research Letters*, 40, 210–215, <https://doi.org/10.1029/2012GL054286>, 2013.
- 285 Alterskjær, K., Kristjánsson, J. E., and Seland, O.: Sensitivity to deliberate sea salt seeding of marine clouds - observations and model simulations, *Atmospheric Chemistry and Physics*, 12, 2795–2807, <https://doi.org/10.5194/acp-12-2795-2012>, 2012.
- Alterskjær, K., Kristjánsson, J. E., Boucher, O., Muri, H., Niemeier, U., Schmidt, H., Schulz, M., and Timmreck, C.: Sea-salt injections into the low-latitude marine boundary layer: The transient response in three Earth system models, *Journal of Geophysical Research-Atmospheres*, 118, 12 195–12 206, <https://doi.org/10.1002/2013JD020432>, 2013.
- 290 Aswathy, N., Boucher, O., Quaas, M., Niemeier, U., Muri, H., Muelmenstaedt, J., and Quaas, J.: Climate extremes in multi-model simulations of stratospheric aerosol and marine cloud brightening climate engineering, *Atmospheric Chemistry and Physics*, 15, 9593–9610, <https://doi.org/10.5194/acp-15-9593-2015>, 2015.
- Bentsen, M., Bethke, I., Debernard, J. B., Iversen, T., Kirkevag, A., Seland, O., Drange, H., Roelandt, C., Seierstad, I. A., Hoose, C., and Kristjánsson, J. E.: The Norwegian Earth System Model, NorESM1-M - Part I: Description and basic evaluation of the physical climate, *Geoscientific Model Development*, 6, 687–720, <https://doi.org/10.5194/gmd-6-687-2013>, 2013.
- 295 Crutzen, P. J.: Albedo enhancement by stratospheric sulfur injections: A contribution to resolve a policy dilemma?, *Climatic Change*, 77, 211–219, <https://doi.org/10.1007/s10584-006-9101-y>, 2006.
- Dagon, K. and Schrag, D. P.: Quantifying the effects of solar geoengineering on vegetation, *Climatic Change*, 153, 235–251, <https://doi.org/10.1007/s10584-019-02387-9>, 2019.
- 300 Gasparini, B., Munch, S., Poncet, L., Feldmann, M., and Lohmann, U.: Is increasing ice crystal sedimentation velocity in geoengineering simulations a good proxy for cirrus cloud seeding?, *Atmospheric Chemistry and Physics*, 17, 4871–4885, <https://doi.org/10.5194/acp-17-4871-2017>, 2017.
- Gent, P. R., Danabasoglu, G., Donner, L. J., Holland, M. M., Hunke, E. C., Jayne, S. R., Lawrence, D. M., Neale, R. B., Rasch, P. J., Vertenstein, M., Worley, P. H., Yang, Z.-L., and Zhang, M.: The Community Climate System Model Version 4, *Journal of Climate*, 24, 4973–4991, <https://doi.org/10.1175/2011JCLI4083.1>, 2011.
- 305 Hurtt, G. C., Chini, L. P., Frolking, S., Betts, R. A., Feddema, J., Fischer, G., Fisk, J. P., Hibbard, K., Houghton, R. A., Janetos, A., Jones, C. D., Kindermann, G., Kinoshita, T., Goldewijk, K. K., Riahi, K., Shevliakova, E., Smith, S., Stehfest, E., Thomson, A., Thornton, P., van Vuuren, D. P., and Wang, Y. P.: Harmonization of land-use scenarios for the period 1500-2100: 600 years of global gridded annual land-use transitions, wood harvest, and resulting secondary lands, *Climatic Change*, 109, 117–161, <https://doi.org/10.1007/s10584-011-0153-2>, 2011.
- 310 IPCC: Climate Change: The Physical Science Basis. Contribution of Working Group I to the Fifth Assessment Report of the Intergovernmental Panel on Climate Change, edited by: Stocker, T. F., Qin, D., Plattner, G.-K., Tignor, M., Allen, S. K., Boschung, J., Nauels, A., Xia, Y., Bex, V., and Midgley, P. M., Cambridge University Press, Cambridge, UK and New York, NY, USA., 2013.
- IPCC: Global warming of 1.5°C. An IPCC Special Report on the impacts of global warming of 1.5°C above pre-industrial levels and related global greenhouse gas emission pathways, in the context of strengthening the global response to the threat of climate change, sustainable development, and efforts to eradicate poverty, V. Masson-Delmotte V., Zhai P., Pörtner H.O., Roberts D., Skea J., Shukla P.R., Pirani A.,



- Moufouma-Okia W., Péan C., Pidcock R., Connors S., Matthews J.B.R., Chen Y., Zhou X., Gomis M.I., Lonnoy E., Maycock M., Tignor M., Waterfield T. (eds.), 2018.
- Irvine, P., Emanuel, K., He, J., Horowitz, L. W., Vecchi, G., and Keith, D.: Halving warming with idealized solar geoengineering moderates key climate hazards, *Nature Climate Change*, 9, 295–299, <https://doi.org/10.1038/s41558-019-0398-8>, 2019.
- Jones, A., Haywood, J. M., Alterskjær, K., Boucher, O., Cole, J. N. S., Curry, C. L., Irvine, P. J., Ji, D., Kravitz, B., Kristjánsson, J. E., Moore, J. C., Niemeier, U., Robock, A., Schmidt, H., Singh, B., Tilmes, S., Watanabe, S., and Yoon, J.-H.: The impact of abrupt suspension of solar radiation management (termination effect) in experiment G2 of the Geoengineering Model Intercomparison Project (GeoMIP), *Journal of Geophysical Research-Atmospheres*, 118, 9743–9752, <https://doi.org/10.1002/jgrd.50762>, 2013.
- Keller, D. P., Feng, E. Y., and Oeschles, A.: Potential climate engineering effectiveness and side effects during a high carbon dioxide-emission scenario, *Nature Communications*, 5, 3304, <https://doi.org/10.1038/ncomms4304>, 2014.
- Kirkevåg, A., Iversen, T., Seland, O., Hoose, C., Kristjánsson, J. E., Struthers, H., Ekman, A. M. L., Ghan, S., Griesfeller, J., Nilsson, E. D., and Schulz, M.: Aerosol-climate interactions in the Norwegian Earth System Model-NorESM1-M, *Geoscientific Model Development*, 6, 207–244, <https://doi.org/10.5194/gmd-6-207-2013>, 2013.
- Kravitz, B., Robock, A., Tilmes, S., Boucher, O., English, J. M., Irvine, P. J., Jones, A., Lawrence, M. G., MacCracken, M., Muri, H., Moore, J. C., Niemeier, U., Phipps, S. J., Sillmann, J., Storelvmo, T., Wang, H., and Watanabe, S.: The Geoengineering Model Intercomparison Project Phase 6 (GeoMIP6): simulation design and preliminary results, *Geoscientific Model Development*, 8, 3379–3392, <https://doi.org/10.5194/gmd-8-3379-2015>, wOS:000364326200024, 2015.
- Kristjánsson, J. E., Muri, H., and Schmidt, H.: The hydrological cycle response to cirrus cloud thinning, *Geophysical Research Letters*, 42, 10 807–10 815, <https://doi.org/10.1002/2015GL066795>, 2015.
- Latham, J.: Control of Global Warming, *Nature*, 347, 339–340, <https://doi.org/10.1038/347339b0>, 1990.
- Lauvset, S. K., Tjiputra, J., and Muri, H.: Climate engineering and the ocean: effects on biogeochemistry and primary production, *Biogeosciences*, 14, 5675–5691, <https://doi.org/10.5194/bg-14-5675-2017>, wOS:000418333700001, 2017.
- Lawrence, D. M., Oleson, K. W., Flanner, M. G., Thornton, P. E., Swenson, S. C., Lawrence, P. J., Zeng, X., Yang, Z.-L., Levis, S., Sakaguchi, K., Bonan, G. B., and Slater, A. G.: Parameterization improvements and functional and structural advances in version 4 of the Community Land Model, *Journal of Advances in Modeling Earth Systems*, 3, 10.1029/2011MS000045, <https://doi.org/10.1029/2011MS000045>, 2011.
- Lawrence, D. M., Oleson, K. W., Flanner, M. G., Fletcher, C. G., Lawrence, P. J., Levis, S., Swenson, S. C., and Bonan, G. B.: The CCSM4 land simulation, 1850–2005: Assessment of surface climate and new capabilities, *Journal of Climate*, 25, 2240–2260, <https://doi.org/10.1175/JCLI-D-11-00103.1>, 2012.
- Lawrence, M. G., Schaefer, S., Muri, H., Scott, V., Oeschles, A., Vaughan, N. E., Boucher, O., Schmidt, H., Haywood, J., and Scheffran, J.: Evaluating climate geoengineering proposals in the context of the Paris Agreement temperature goals, *Nature Communications*, 9, 3734, <https://doi.org/10.1038/s41467-018-05938-3>, 2018.
- Lee, H., Ekici, A., Tjiputra, J., Muri, H., Chadburn, S. E., Lawrence, D. M., and Schwinger, J.: The response of permafrost and high-latitude ecosystems under large-scale stratospheric aerosol injection and its termination, *Earth's Future*, 7, 605–614, <https://doi.org/https://doi.org/10.1029/2018EF001146>, 2019.
- Li, J.-L. F., Waliser, D. E., Chen, W.-T., Guan, B., Kubar, T., Stephens, G., Ma, H.-Y., Deng, M., Donner, L., Seman, C., and Horowitz, L.: An observationally based evaluation of cloud ice water in CMIP3 and CMIP5 GCMs and contemporary reanalyses using contemporary satellite data, *Journal of Geophysical Research-Atmospheres*, 117, D16 105, doi:10.1029/2012JD017640, <https://doi.org/10.1029/2012JD017640>, 2012.



- 355 Mercado, L. M., Bellouin, N., Sitch, S., Boucher, O., Huntingford, C., Wild, M., and Cox, P. M.: Impact of changes in diffuse radiation on the global land carbon sink, *Nature*, 458, 1014–U87, <https://doi.org/10.1038/nature07949>, 2009.
- Mitchell, D.: Use of mass- and area-dimensional power laws for determining precipitation particle terminal velocities, *Journal of the Atmospheric Sciences*, 53, 1710–1723, [https://doi.org/10.1175/1520-0469\(1996\)053<1710:UOMAAD>2.0.CO;2](https://doi.org/10.1175/1520-0469(1996)053<1710:UOMAAD>2.0.CO;2), 1996.
- Muri, H., Kristjánsson, J. E., Storelvmo, T., and Pfeffer, M. A.: The climatic effects of modifying cirrus clouds in a climate engineering framework, *Journal of Geophysical Research-Atmospheres*, 119, 4174–4191, <https://doi.org/10.1002/2013JD021063>, 2014.
- 360 Muri, H., Tjiputra, J., Otterå, O. H., Adakudlu, M., Lauvset, S. K., Grini, A., Schulz, M., Niemeier, U., and Kristjánsson, J. E.: Climate response to aerosol geoengineering: A multimethod comparison, *J. Climate*, 31, 6319–6340, <https://doi.org/10.1175/JCLI-D-17-0620.1>, <https://doi.org/10.1175/JCLI-D-17-0620.1>, 2018.
- Naik, V., Wuebbles, D., DeLucia, E., and Foley, J.: Influence of geoengineered climate on the terrestrial biosphere, *Environmental Management*, 32, 373–381, <https://doi.org/10.1007/s00267-003-2993-7>, 2003.
- 365 Niemeier, U. and Timmreck, C.: What is the limit of climate engineering by stratospheric injection of SO₂?, *Atmospheric Chemistry and Physics*, 15, 9129–9141, <https://doi.org/10.5194/acp-15-9129-2015>, 2015.
- Niemeier, U., Schmidt, H., and Timmreck, C.: The dependency of geoengineered sulfate aerosol on the emission strategy, *Atmospheric Science Letters*, 12, 189–194, <https://doi.org/10.1002/asl.304>, 2011.
- 370 Parker, A. and Irvine, P. J.: The Risk of Termination Shock From Solar Geoengineering, *Earth's Future*, 6, 456–467, <https://doi.org/10.1002/2017EF000735>, 2018.
- Ramankutty, N. and Foley, J.: Estimating historical changes in global land cover: Croplands from 1700 to 1992, *Global Biogeochemical Cycles*, 13, 997–1027, <https://doi.org/10.1029/1999GB900046>, 1999.
- Riahi, K., Rao, S., Krey, V., Cho, C., Chirkov, V., Fischer, G., Kindermann, G., Nakicenovic, N., and Rafaj, P.: RCP 8.5—A scenario of comparatively high greenhouse gas emissions, *Climatic Change*, 109, 33. <https://doi.org/10.1007/s10584-011-0149-y>, <https://doi.org/10.1007/s10584-011-0149-y>, 2011.
- 375 Robock, A.: Albedo enhancement by stratospheric sulfur injections: More research needed, *Earth's Future*, 4, 644–648, <https://doi.org/10.1002/2016EF000407>, 2016.
- Robock, A., Marquardt, A., Kravitz, B., and Stenchikov, G.: Benefits, risks, and costs of stratospheric geoengineering, *Geophysical Research Letters*, 36, L19 703, doi:10.1029/2009GL039 209, <https://doi.org/10.1029/2009GL039209>, 2009.
- 380 Rogelj, J., den Elzen, M., Hoehne, N., Fransen, T., Fekete, H., Winkler, H., Chaeffer, R. S., Ha, F., Riahi, K., and Meinshausen, M.: Paris Agreement climate proposals need a boost to keep warming well below 2 degrees C, *Nature*, 534, 631–639, <https://doi.org/10.1038/nature18307>, wOS:000378676000026, 2016.
- Rogelj, J., Popp, A., Calvin, K. V., Luderer, G., Emmerling, J., Gernaat, D., Fujimori, S., Streffer, J., Hasegawa, T., Marangoni, G., Krey, V., Kriegler, E., Riahi, K., van Vuuren, D. P., Doelman, J., Drouet, L., Edmonds, J., Fricko, O., Harmsen, M., Havlik, P., Humpenoeder, F., Stehfest, E., and Tavoni, M.: Scenarios towards limiting global mean temperature increase below 1.5 degrees C, *Nature Climate Change*, 8, 325–332, <https://doi.org/10.1038/s41558-018-0091-3>, 2018.
- 385 Schäfer, S., Lawrence, M., Stelzer, H., Born, W., and Low, S.: The European Transdisciplinary Assessment of Climate Engineering (EuTRACE), Final Rep. of the FP7 CSA Project EuTRACE, Tech. rep., Institute for Advanced Sustainability Studies (IASS), Potsdam, Germany, 2015.
- 390



- Stjern, C. W., Muri, H., Ahlm, L., Boucher, O., Cole, J. N. S., Ji, D., Jones, A., Haywood, J., Kravitz, B., Lenton, A., Moore, J. C., Niemeier, U., Phipps, S. J., Schmidt, H., Watanabe, S., and Kristjánsson, J. E.: Response to marine cloud brightening in a multi-model ensemble, *Atmospheric Chemistry and Physics*, 18, 621–634, <https://doi.org/10.5194/acp-18-621-2018>, 2018.
- 395 Storelvmo, T., Kristjánsson, J. E., Muri, H., Pfeffer, M., Barahona, D., and Nenes, A.: Cirrus cloud seeding has potential to cool climate, *Geophysical Research Letters*, 40, 178–182, <https://doi.org/10.1029/2012GL054201>, 2013.
- Thomson, A. M., Calvin, K. V., Smith, S. J., Kyle, G. P., Volke, A., Patel, P., Delgado-Arias, S., Bond-Lamberty, B., Wise, M. A., Clarke, L. E., and Edmonds, J. A.: RCP4.5: a pathway for stabilization of radiative forcing by 2100, *Climatic Change*, 109, 77–94, <https://doi.org/10.1007/s10584-011-0151-4>, wOS:000297350200005, 2011.
- Thornton, P. E., Doney, S. C., Lindsay, K., Moore, J. K., Mahowald, N., Randerson, J. T., Fung, I., Lamarque, J. F., Feddema, J. J., and Lee, Y. H.: Carbon-nitrogen interactions regulate climate-carbon cycle feedbacks: results from an atmosphere-ocean general circulation model, *Biogeosciences*, 6, 2099–2120, <https://doi.org/10.5194/bg-6-2099-2009>, 2009.
- 400 Tilmes, S., Mills, M. J., Niemeier, U., Schmidt, H., Robock, A., Kravitz, B., Lamarque, J. F., Pitari, G., and English, J. M.: A new Geoengineering Model Intercomparison Project (GeoMIP) experiment designed for climate and chemistry models, *Geoscientific Model Development*, 8, 43–49, <https://doi.org/10.5194/gmd-8-43-2015>, 2015.
- 405 Tjiputra, J. F., Roelandt, C., Bentsen, M., Lawrence, D. M., Lorentzen, T., Schwinger, J., Seland, O., and Heinze, C.: Evaluation of the carbon cycle components in the Norwegian Earth System Model (NorESM), *Geoscientific Model Development*, 6, 301–325, <https://doi.org/10.5194/gmd-6-301-2013>, 2013.
- Tjiputra, J. F., Grini, A., and Lee, H.: Impact of idealized future stratospheric aerosol injection on the large-scale ocean and land carbon cycles, *Journal of Geophysical Research-Biogeosciences*, 121, 2–27, <https://doi.org/10.1002/2015JG003045>, 2016.
- 410 UNFCCC: Adoption of the Paris Agreement United Nations Framework Convention on Climate Change, Geneva: United Nations Office, 2015.
- van Vuuren, D. P., Edmonds, J., Kainuma, M., Riahi, K., Thomson, A., Hibbard, K., Hurtt, G. C., Kram, T., Krey, V., Lamarque, J.-F., Masui, T., Meinshausen, M., Nakicenovic, N., Smith, S. J., and Rose, S. K.: The representative concentration pathways: an overview, *Climatic Change*, 109, 5–31, <https://doi.org/10.1007/s10584-011-0148-z>, 2011.
- 415 van Vuuren, D. P., Stehfest, E., Gernaat, D. E. H. J., van den Berg, M., Bijl, D. L., de Boer, H. S., Daioglou, V., Doelman, J. C., Edelenbosch, O. Y., Harmsen, M., Hof, A. F., and van Sluisveld, M. A. E.: Alternative pathways to the 1.5 degrees C target reduce the need for negative emission technologies, *Nature Climate Change*, 8, 391–397, <https://doi.org/10.1038/s41558-018-0119-8>, 2018.
- Wei, L., Ji, D., Miao, C., Muri, H., and Moore, J. C.: Global streamflow and flood response to stratospheric aerosol geoengineering, *Atmospheric Chemistry and Physics*, 18, 16 033–16 050, <https://doi.org/10.5194/acp-18-16033-2018>, 2018.
- 420 Yu, X., Moore, J. C., Cui, X., Rinke, A., Ji, D., Kravitz, B., and Yoon, J.-H.: Impacts, effectiveness and regional inequalities of the GeoMIP G1 to G4 solar radiation management scenarios, *Global and Planetary Change*, 129, 10–22, <https://doi.org/10.1016/j.gloplacha.2015.02.010>, 2015.
- Zickfeld, K., Solomon, S., and Gilford, D. M.: Centuries of thermal sea-level rise due to anthropogenic emissions of short-lived greenhouse gases, *Proc Natl Acad Sci USA*, 114, 657, <https://doi.org/10.1073/pnas.1612066114>, 2017.

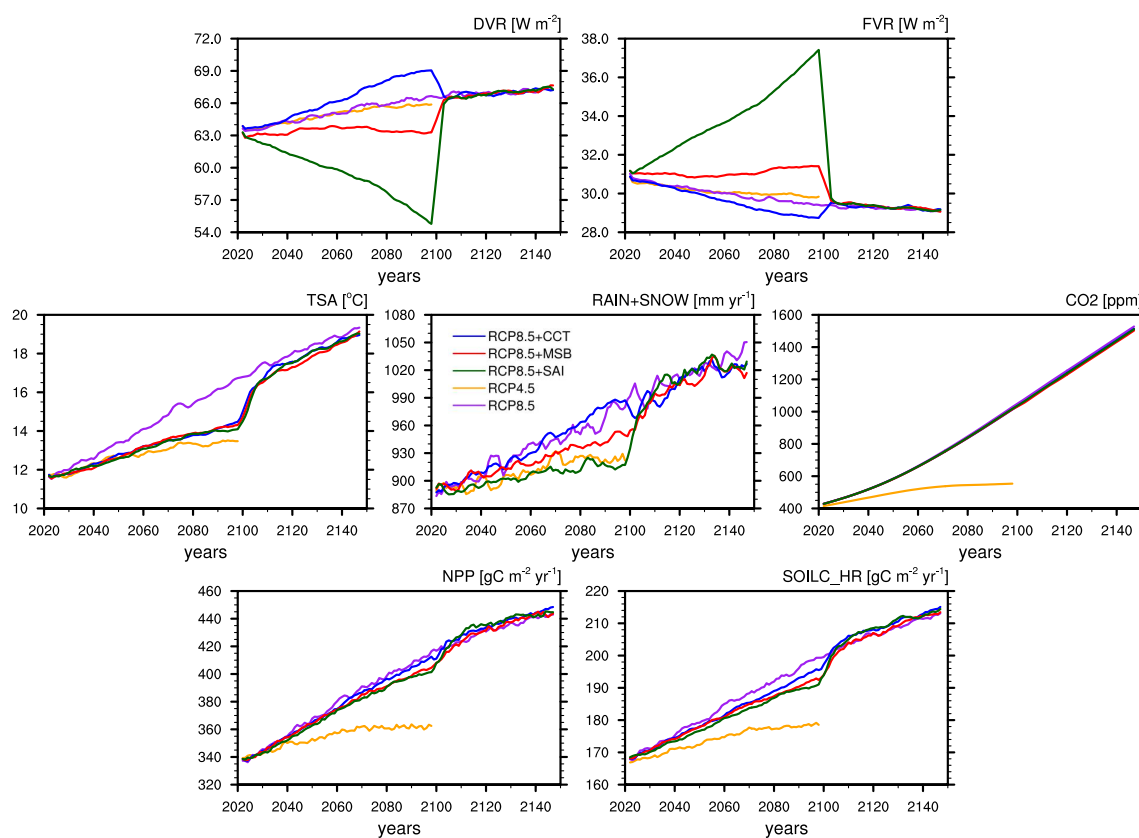


Figure 1. Time-series of changes in land surface mean radiation, CO₂, air temperature, precipitation, NPP, and soil carbon release from RCP4.5, RCP8.5, CCT, MSB, and SAI simulations. The values shown here are -60 to 70°N mean from land area.

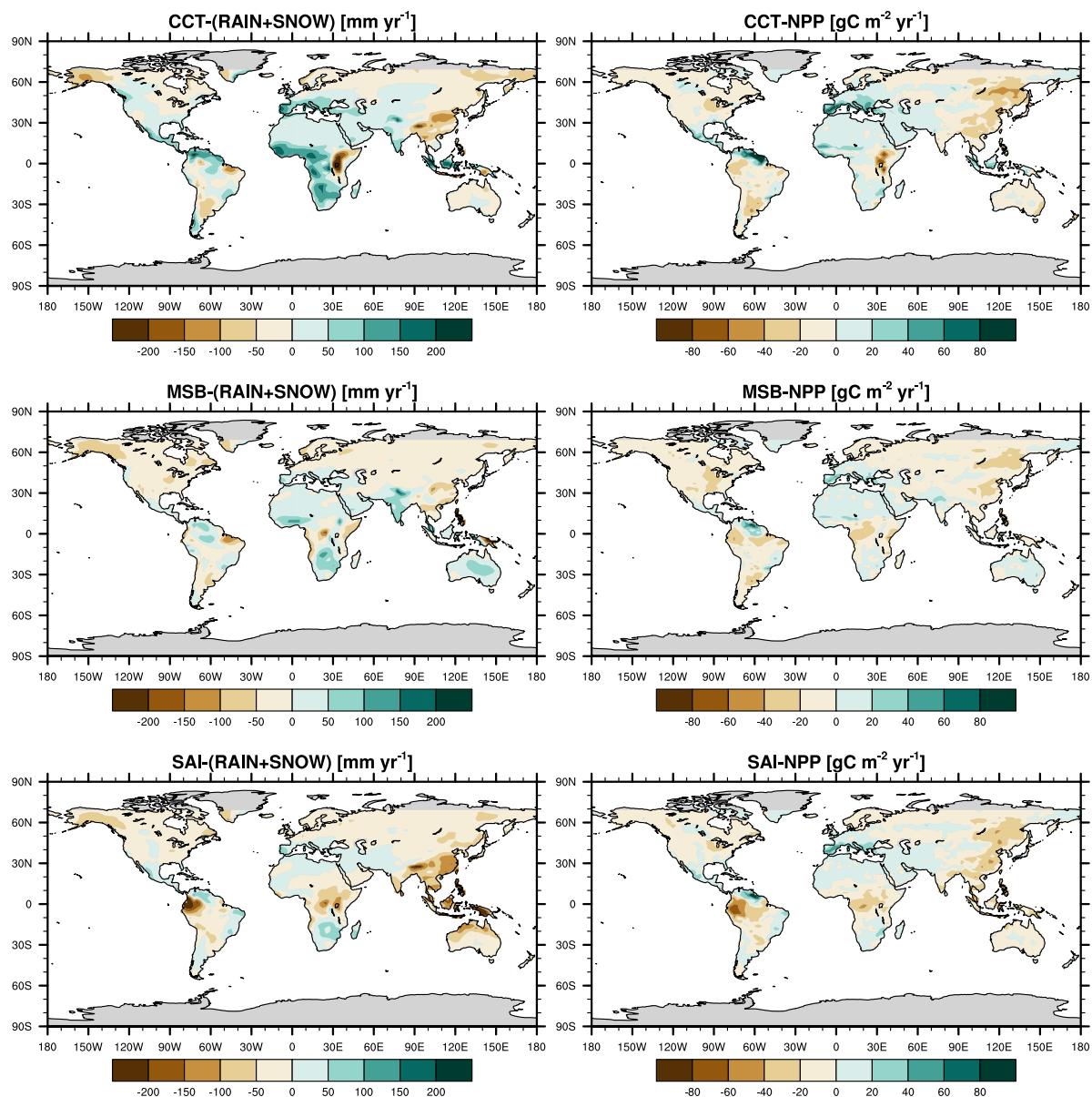


Figure 2. The spatial patterns in the deviation of precipitation and NPP simulated by CCT, MSB, and SAI relative to the baseline RCP8.5 scenario. The values shown here are the mean difference of the 2070-2100 time period and the mean over three ensemble members.

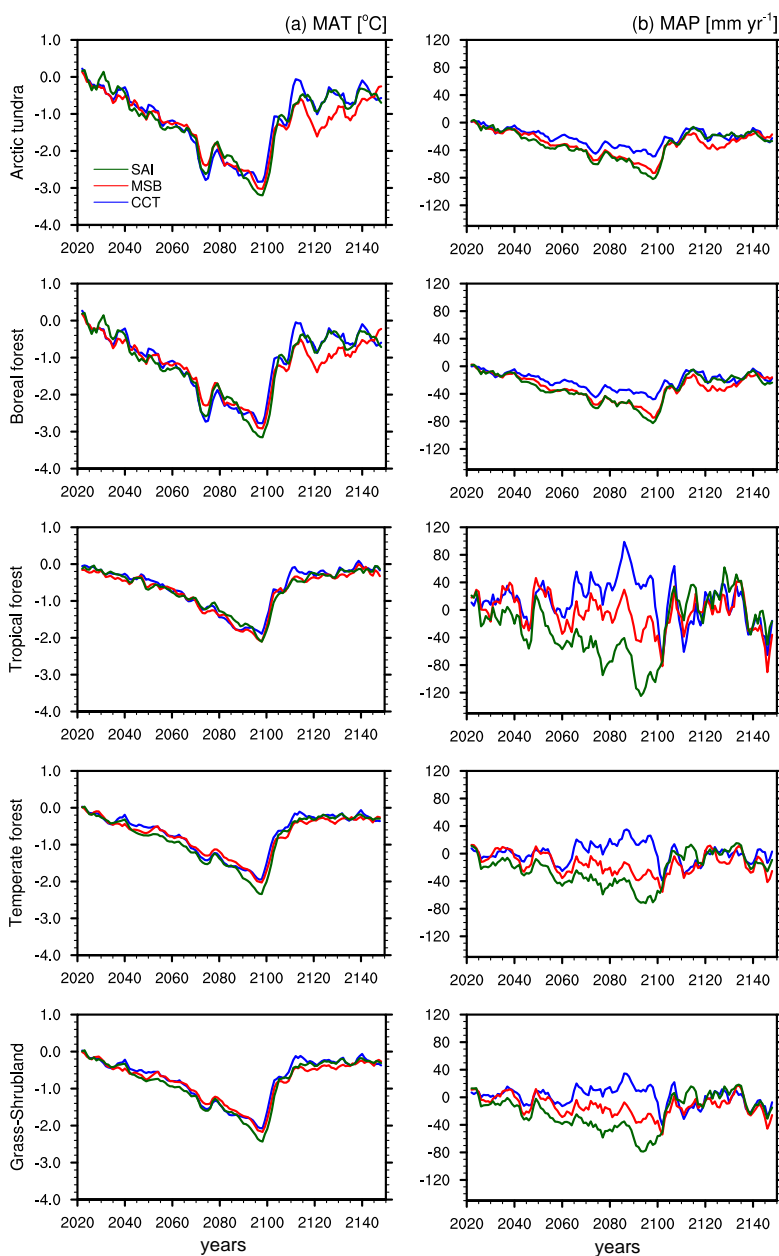


Figure 3. Mean annual temperature and precipitation in five different land biomes (-60-70°N). The changes are relative to the baseline RCP8.5 scenario.

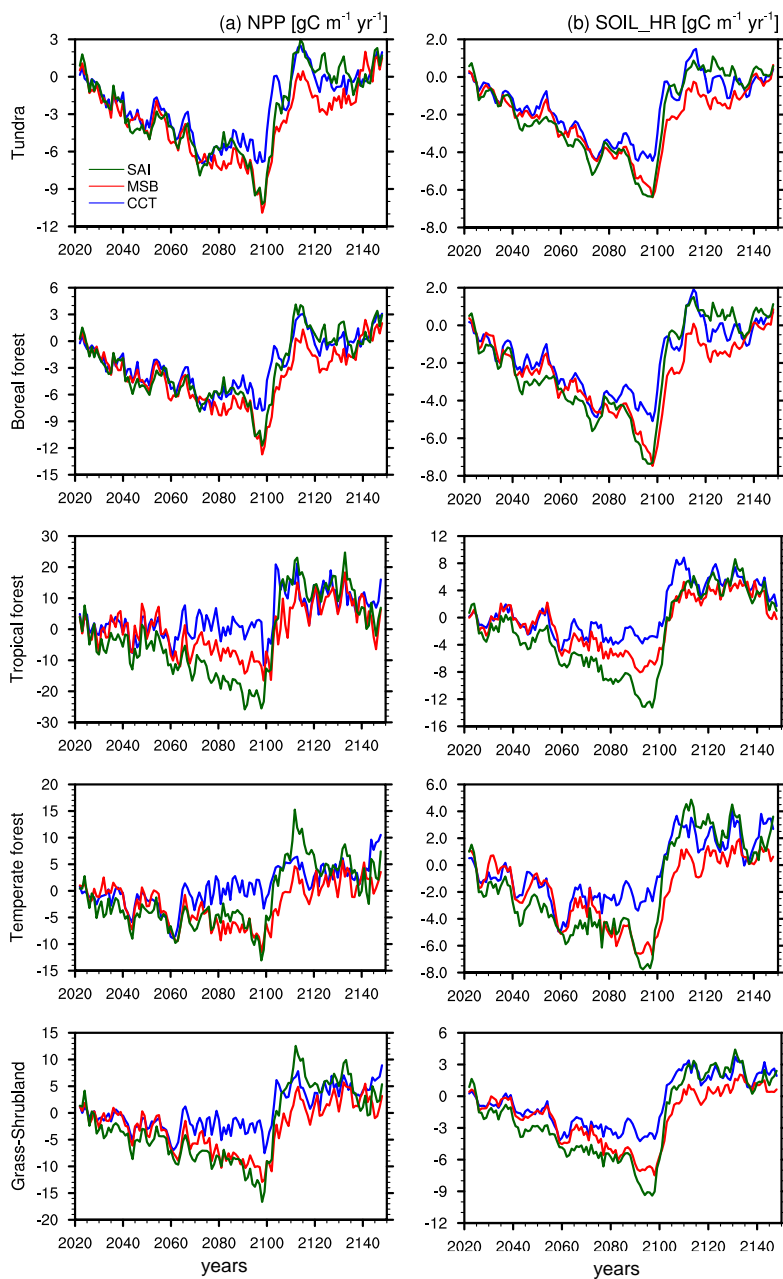


Figure 4. The relative difference between the RM to RCP8.5 scenario. The values are mean biome NPP and SOIL_HR in -60 to 70°N.

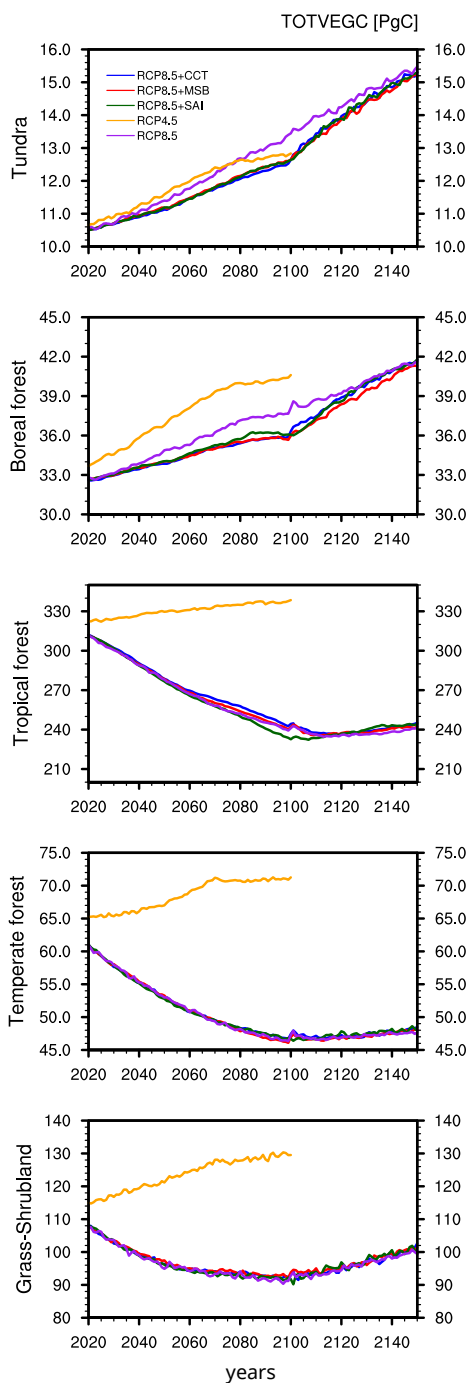


Figure 5. Total vegetation carbon storage in five different biomes under simulations of RCP8.5, three RM methods applied on top of RCP8.5 climate forcing (CCT, MSB, and SAI), and RCP4.5 scenarios.